Chapter IV

DATA

IV.A. Observations

The observing schedule of CGRO is organized in so-called Phases, each approximately a year in duration. Each Phase consists of scheduled viewing periods (VP) that are typically 1–2 weeks of pointed observations. The scheduled sequence of VPs were occasionally interrupted to allow for Target-of-Opportunity observations. After the all-sky survey conducted in Phase 1 (April 1991–November 1992), the scheduled VPs consisted of targeted observations of regions of special interest. Select regions such as the Galactic center, the Anticenter region, the Cygnus region and the Virgo region were observed several times.

Two criteria are applied in selecting observations for the CDG analysis: first that the pointing be far from the Galactic plane and second (less important) that the pointing directions lie along the orbital plane. In general, all of the COMPTEL data contain the diffuse Galactic component at some level. Since the Galactic emission rapidly drops in intensity far above and below the plane, the high-Galactic latitude observations are chosen for the CDG analysis in order to minimize this contribution. Pointings that lie along the orbital plane have long periods of time when the Earth is completely outside the COMPTEL field-of-view.

The Virgo direction satisfies both these criteria, the Virgo pointings have a galactic latitude ranging from 60 to 70˚ with declination around 1–10˚. In addition, COMPTEL has performed numerous observations of the Virgo direction making it the ideal dataset for CDG studies. Here I use the data from all of the Phase 1 through Phase 5 observations of the Virgo direction, tabulated below in table IV.1. A total of 169 days of pointed COMPTEL observations.

Table IV.1 The Virgo observations ([†]Truncated Julian Date = Julian date – 2440000.0; [§]Galactic longitude; [‡]Galactic latitude).

Phase	VP	TJD[†]	$l^{\S}$ pointing	$b^{\ddagger}$ pointing
1	3	8422–8435	300.02	65.43
1	11	8532–8546	294.48	63.64
2	204	8978–8985	294.64	61.88
2	205	8985–8986, 8988–8992	294.53	61.59
2	206	8992–8993, 8995–8999	294.64	61.87
3	304	9279–9285	278.2	66.68
3	305	9285–9293	277.7	62.69
3	306	9293–9300	277.58	58.7
3	307	9300–9307	268.61	69.27
3	308	9307–9310, 9315–9322	283.26	74.65
3	311	9334–9336, 9339–9341	283.7	74.5
3	312	9341–9348	280.72	70.73
3	313	9348–9355	289.19	78.7
4	405	9685–9693	306.71	56.55
4	406	9699–9706	336.44	67.22
4	407	9706–9720	334.35	62.98
4	408	9720–9727	305.17	57.07
5	511	10098–10112	298.37	62.89
5	511.5	10112-10119	310.61	53.18

To serve as a second independent dataset, data from several observations towards the South Galactic Pole (SGP) were analyzed. For these data, most pointing directions with Galactic latitudes lower than roughly –50˚ were accepted. This criteria selected many viewing periods from Phases 1, 4 and 5 (the other phases had little exposure towards the SGP). The SGP data provide 97 days of pointed COMPTEL observations, tabulated below in table IV.2.

The observed Virgo and SGP regions represent large areas towards the North and South Galactic poles, respectively. They are used separately to investigate any large scale inhomogeneity in the inferred CDG emission. The pointing directions for the Virgo and SGP data in the individual phases are shown in figure IV.1–4. The circle represents the 40˚ field-of-view cut (discussed below) imposed on sky viewing for CDG analysis.

Table IV.2 The SGP observations.

Phase	VP	TJD	*l* pointing	*b* pointing
1	9	8504–8511	338.83	-83.53
1	10	8518–8532	287.77	-54.33
1	13.5	8567–8574	338.75	-83.58
4	404	9671–9685	7.15	-73.45
4	428	9967–9980	270.46	-82.45
5	513	10119–10126	17.56	-52.16
5	514	10126–10133	62.28	-60.63
5	517	10147–10160	276.83	-59.53
5	520.4	10224–10231	17.71	-52.27

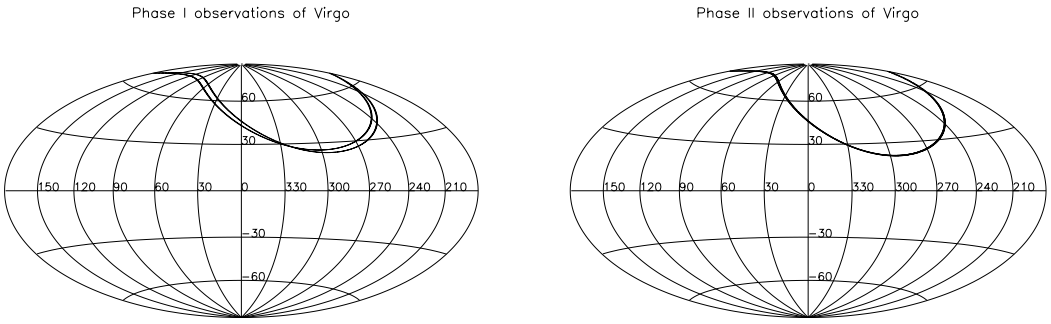

Figure IV.1 The Phase 1 and Phase 2 Virgo observations.

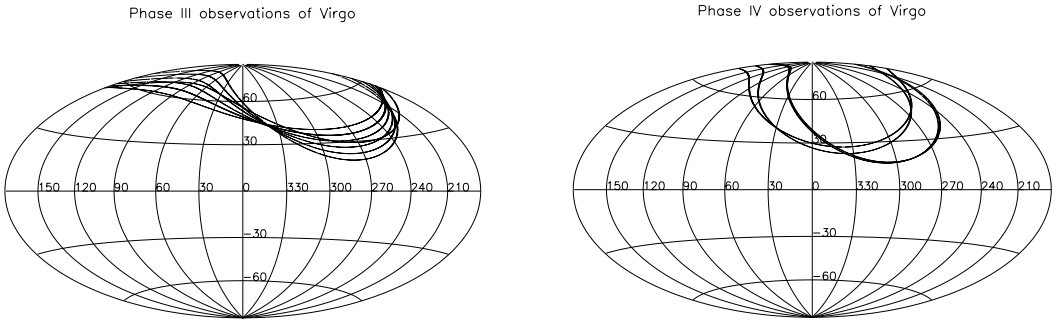

Figure IV.2 The Phase 3 and Phase 4 Virgo observations.

Each of the 21 modules in the D1 and D2 detectors can be independently switched on or off, thereby altering the instrument geometry that strongly effects the instrument response. All the data accumulated in this analysis during and after Phase II have the same D1-D2 module settings (the D2-1 and D2-2 modules switched off). During Phase I there were many changes in the instrument configuration, leading to three distinct D1-D2 settings (table IV.3).

Table IV.3 The instrument geometry for the Virgo and SGP observations.

Phase	VP	TJD start	TJD end	D1 OFF	D2 OFF
1	3	8422	8426	–	5, 14
1	3	8427	8435	–	14
1	11	8432	8546	4	14
1	9	8504	8511	4	14
1	10	8518	8532	4	14
1	13.5	8567	8574	4	14
2+	all	–	–	–	1, 2

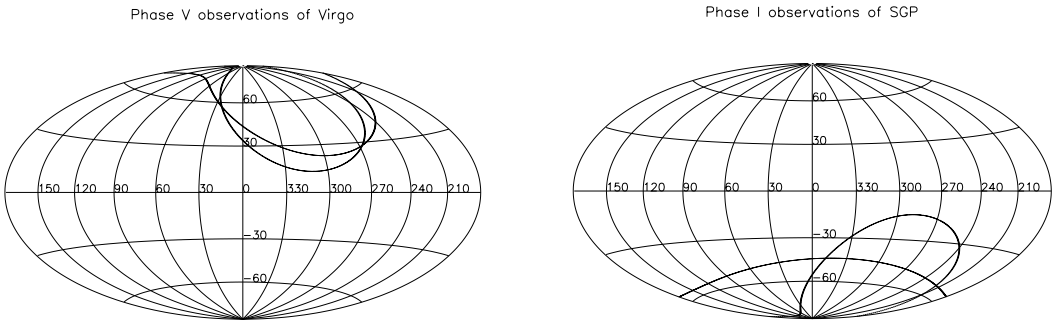

Figure IV.3 The Phase 5 Virgo and Phase 1 SGP observations.

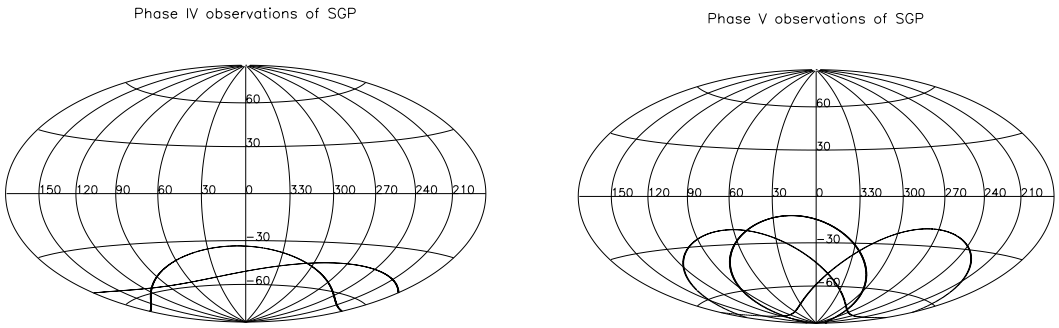

Figure IV.4 The Phase 4 and Phase 5 SGP observations.

Many different subsets of the Virgo and SGP data were analyzed separately for this work. These are listed in table IV.4. The total Virgo dataset is separated into three time intervals, namely, Phases 1 & 2 combined (P12V), Phase 3 (P3V) and Phases 4 & 5 combined (P45V). The SGP dataset is separated into two time intervals, namely, Phase 1 (P1SGP) and Phases 4 and 5 combined (P45SGP). With such a separation we get five independent datasets. I have combined the Virgo Phases 1 & 2 and Phases 4 & 5 data to produce datasets with comparable

statistics. Since the Virgo Phase 2 and Phase 5 data have smaller exposures, their ToF spectra have poor statistics. Likewise the SGP Phases 4 & 5 were combined to improve statistics.

Table IV.4 Terminology used for the different datasets.

Name	Data description
P15VSGP	all Virgo and all SGP data
P12345V	all Virgo data
P2345V	Phases 2 to 5 Virgo data
P145SGP	all SGP data
P12V	Phases 1 and 2 Virgo data
P3V	Phase 3 Virgo data
P45V	Phases 4 and 5 Virgo data
P1SGP	Phase 1 SGP data
P45SGP	Phases 4 and 5 SGP data
P23a	Phases 2 and pre-reboost 3 Virgo data

IV.B. Removal of Atmospheric Gamma Rays

Typically, the COMPTEL sky is occulted by the Earth once per orbit. The Earth is an intense source of gamma rays and subtends a large area of the sky (70˚ wide radius at the nominal orbit altitude of 450 km). These atmospheric gamma rays are a strong background source. The data used in this analysis were accumulated during the periods when the Earth was outside the COMPTEL field-of-view. This is achieved through a combination of observation-time selections (EHORA cuts) and event-geometry selections (event-circle cuts). The exact prescription for the removal of the Earth from the field-of-view is described below. First some important definitions:

- The scatter-direction of the photon, **S** is defined as the vector passing through the photon interaction locations D1 and D2.
- Let η be defined as the angle between the COMPTEL *z*-axis (the pointing direction) and the scatter-direction **S** of the incident photon.
- The spacecraft-Earth Horizon Angle (EHORA) is defined as the angle between the *z*-axis and the nearest point of the Earth's horizon.

For a given altitude the Earth has a fixed angular diameter. The EHORA is computed as the difference between the GCEL angle and the Earth's angular radius. It is negative when the *z*-axis is pointed into the Earth (see figure IV.7). Hence for a given altitude (when the

apparent Earth-radius is fixed) there is a one-to-one correspondence between EHORA and GCEL. The EHORA-GCEL correlation is shown in figure IV.6.

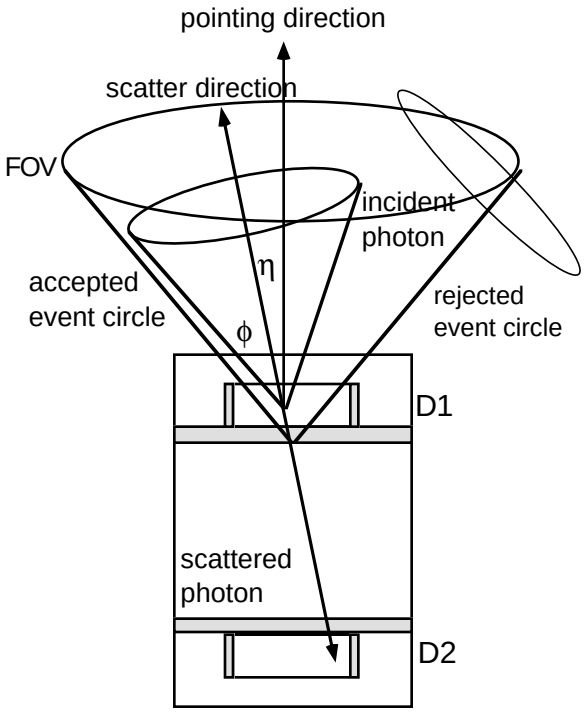

Figure IV.5 A schematic of the CDG field-of-view selection.

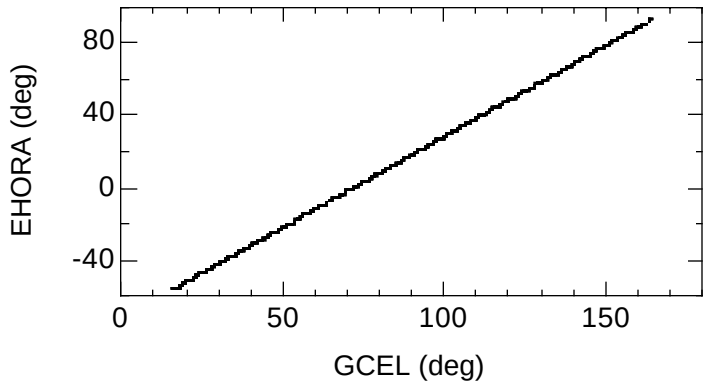

Figure IV.6 The correlation between the EHORA and the GCEL angles for TJD 9725.

If we assume that all events undergo a single Compton-scatter in the D1 detector then each detected photon originates somewhere along an event-circle of radius ϕ centered about the scatter-direction **S**. The uncertainties in the measured interaction locations and the measured energy deposits lead to uncertainties in the computed scatter-angle ϕ, broadening the measured event circle.

We only accept events that satisfy the relation $\phi + \eta \leq 40^\circ$. The entire event-circle of each accepted event is now completely contained within 40˚ of the pointing direction. This forces all accepted events to originate within 40˚ of the pointing direction (*z*-axis). The COMPTEL field-of-view (FoV) is now strictly a 40˚ circle (1.47 sr) about the pointing-direction. This FoV selection is achieved through data selections that depend on event parameter only.

We now accumulate data only during times when EHORA > 45˚. This additional criteria now forces the Earth's horizon to be always more than 45˚ from the pointing-direction or equivalently, the Earth's horizon is always more than 5˚ from the edge of the FoV. All of the atmospheric photons will now have event circles that pass through regions >45˚ from the pointing direction. This is a selection on orbital data and independent of any event parameter.

Therefore, if we accept only those events that totally originate within 40˚ of the pointing direction and if we accumulate data only when the Earth's horizon is greater than 45˚ from the pointing-direction, then there is no contamination of the events within the FoV by the atmospheric photons. The instrument response under these conditions has no Earth-geometry dependence.

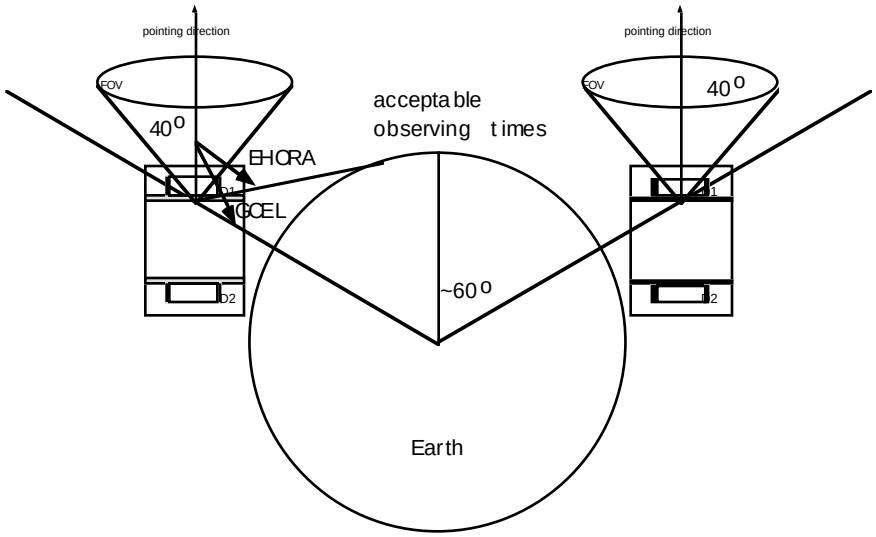

Figure IV.7 A schematic of the COMPTEL orbital and field-of-view selections.

The uncertainties in ϕ do not compromise the effectiveness in rejecting atmospheric photons. Below 10 MeV most events experience escaping energy from D2, resulting in a measured ϕ value larger than the true scatter angle or a positive ARM measurement (see

section II.D). Therefore, these events will originate from within the FoV and are of no concern.

Above 10 MeV, the fraction of events with escaping energy from D1 increases (~20%). The measured ϕ value for these events are smaller than the true scatter angle or a negative ARM measurement (see section II.D). Therefore, events with energy loss in D1 could originate from outside the FoV. The contributions of these events originating from the sky are accounted for in the CDG response calculation.

The potentially problematic case arises only when the photons originate from the Earth's atmosphere when the Earth is just outside the FoV. This is a negligible effect because: (1) EHORA > 5˚ from the edge of the FoV; (2) the number of events with ARM less than 5˚ is <1% below 10 MeV and <5% between 10–30 MeV; (3) EHORA = 45˚ only for a short amount of time during an observation. Therefore, there is negligible contamination from the atmosphere.

At the nominal altitude of 450 km, an EHORA 45˚ corresponds to a GCEL 115˚. Therefore, the EHORA selection of ±45˚ roughly selects approximately 1/3 of each orbit for CDG measurement times. For sky-viewing times, the combined effects of EHORA and FoV selections result in daily CDG EVP datasets of only 17–25% of the original EVP size.

IV.C. Standard-CDG Data Selections

To optimize the signal-to-background in the measurements, a set of specialized selections have been applied to the data. These data selection are describe below and are usually referred to as the *standard-CDG* data selections. These selections are somewhat different from the usual selections defined by the COMPTEL collaboration used in the standard COMPTEL data analysis.

As mentioned before, the event-data (EVP) used for CDG analysis is the Gamma-1 EVP data with the latest ToF (TCFCOR) corrections. To these EVP data we apply the following selections.

Total energy, ETOT : 800–30000 keV

D1 Energy deposit, E1 : 70–20000 keV

D2 Energy deposit, E2: 730–30000 keV

Pulse-shape-discriminator, PSD : 65–95 channels

Scatter angle, ϕ : 6–38°

Sum of scatter angle and scatter-direction angle, $\phi + \eta$: $\leq 40^\circ$

Livetime : > 61%

Here is a brief rationale for the above data selections. The upper energy bound is due to the inadequate knowledge of the instrument response above those energies. The lower bounds on the energy deposits are chosen so as to be above the detector thresholds of each of the individual modules. It is important to realize that the detector thresholds have slowly increased over time and also vary slightly from detector to detector (especially for the D2 detectors). The relatively higher D2 energy threshold used here (compared to E2 > 650 keV cut for the standard selection) is an attempt to minimize the influence of these threshold variations in determining the instrument response. The PSD selections are made to reject neutron-scatter events in D1 which are typically found above channel 95 in PSD. Since electrons (from gamma-ray scatters) produce the fastest decay pulse and lie around channel 80 in PSD, events with a PSD value lower than ~65 (though much fewer in number) are suspect events and therefore rejected. The instrument livetime is on average around 90–95% for sky observations with the above data selections. However, the livetime may occasionally degrade in special circumstances (e.g., for low rigidities following a SAA passage). The selection on livetime of >61% eliminates periods when the uncertainties in the livetime calculation can get large. The FoV cut of ($\phi + \eta \leq 40^\circ$) necessarily imposes a $\phi \leq 40^\circ$ selection.